

RESEARCH

Open Access



Ethanol extract of *Nymphaea lotus* Linn. inhibited hepatic fibrogenesis in carbon tetrachloride-intoxicated Wistar rats

Ifeoluwa Temitayo Oyeyemi^{1*}, Isaac Ayodeji Adesina², Kabirat Adedunmola Sulaiman¹,
Ifeoluwa Temitope Ajayi^{3,5} and Enivwenaye Egide Williams Nabofa⁴

Abstract

Background *Nymphaea lotus* is a plant used as food and to manage various ailments including liver diseases. Liver fibrosis is a pathological state which progresses to more chronic and fatal liver diseases but without any approved drug yet. This study thus aimed to investigate the anti-liver fibrosis mechanism of *N. lotus*.

Methodology Liver fibrosis was induced by carbon tetrachloride (CCl₄:Olive oil, 1:1 ip). Fibrotic animals were treated with 50, 100 and 200 mg/kg b.wt. *N. lotus* extract. The activities of alanine aminotransaminase (ALT), aspartate aminotransferase (AST), in the serum, and levels of Malondialdehyde (MDA), superoxide dismutase (SOD), catalase, and reduced glutathione (GSH) in the liver, and histopathology of the liver were determined. The expression of fibrosis-related proteins namely alpha-smooth muscle actin (α -SMA), Collagen-4 (COL4A), Transforming growth factor- β 1 (TGF β 1), Mothers against decapentaplegic homolog 2 (SMAD2), SMAD3 and matrix metalloproteinase 2 (MMP2) in the liver was also evaluated. Molecular docking and simulation analysis of *N. lotus*-derived phytochemicals to TGF β 1 and SMAD3 was also performed.

Results The extract significantly reduced the levels of ALT, AST, and MDA, increased the expression of antioxidant enzymes namely; SOD and GSH, and downregulated the expression of fibrosis-related proteins namely α -SMA, COL4A, TGF β 1, SMAD3 and MMP2. It also ameliorated CCl₄-induced hepatic lesions. *N. lotus*-derived phytochemicals also showed a good binding affinity and interaction with the active sites of TGF β 1 and SMAD3.

Conclusion *N. lotus* inhibited liver fibrosis by inhibiting oxidative stress and the TGF β /SMAD signalling pathway. This demonstrates its beneficial and protective effect against CCl₄-induced hepatotoxicity and thus supports its use for the traditional management of liver diseases.

Keywords Liver fibrosis, TGF β /SMAD signalling, Carbon tetrachloride, Oxidative stress, *Nymphaea lotus*

*Correspondence:

Ifeoluwa Temitayo Oyeyemi
ioyeyemi@unimed.edu.ng

Full list of author information is available at the end of the article



© The Author(s) 2024. **Open Access** This article is licensed under a Creative Commons Attribution 4.0 International License, which permits use, sharing, adaptation, distribution and reproduction in any medium or format, as long as you give appropriate credit to the original author(s) and the source, provide a link to the Creative Commons licence, and indicate if changes were made. The images or other third party material in this article are included in the article's Creative Commons licence, unless indicated otherwise in a credit line to the material. If material is not included in the article's Creative Commons licence and your intended use is not permitted by statutory regulation or exceeds the permitted use, you will need to obtain permission directly from the copyright holder. To view a copy of this licence, visit <http://creativecommons.org/licenses/by/4.0/>.

Background

Liver diseases continue to be a major global concern, causing over two million deaths annually, accounting for one in four deaths worldwide, despite ongoing efforts to combat them [1]. Liver fibrosis is a pathological condition that arises from chronic liver injury and sustained activation of inflammation and fibrogenesis [2]. If left untreated, liver fibrosis progresses to more life-threatening conditions such as cirrhosis and hepatocellular carcinoma, which are responsible for the majority of deaths from liver diseases [1, 2].

Liver fibrosis is a dynamic process that tilts the balance of extracellular matrix deposition and degradation resulting in excessive extracellular matrix (ECM) deposition [3] which are regulated by matrix metalloproteinases (MMPs) and their inhibitors – tissue inhibitors of matrix metalloproteinases (TIMPs) [4]. Activation of the hepatic stellate cells (HSC) is crucial to the progression of liver fibrosis. It alters the architecture of the liver thereby impacting its functions [5]. Lipid peroxidation promotes HSC activation and plays a key role in the pathogenesis of liver fibrosis via the production of oxidative stress, transforming growth factor- β (TGF- β), and tumour necrosis factor-alpha (TNF- α) [6, 7].

TGF- β 1 plays a major role in the progression of liver fibrosis. In the presence of injury and inflammation, it induces apoptosis, prevents hepatocyte proliferation, and activates HSCs [8]. It further activates its downstream SMAD signaling which provokes the overexpression of pro-fibrotic cytokines [9]. The TGF- β 1/SMAD signalling pathway is so crucial to the progression of liver fibrosis that the ability to regulate the TGF- β 1/SMAD signalling pathway has become an important test in investigating the efficacy of potential antifibrotic agents [10, 11].

Liver fibrosis is a reversible condition [12] but there are still limited treatment options for treating it. Medicinal plants and/or their isolated compounds have, however, shown promise as therapeutic agents for liver fibrosis. *Nymphaea lotus* is an aquatic food and medicinal plant widely distributed in the tropics. It is used traditionally for the management of different diseases, including liver diseases. It is rich in phytochemicals such as tannins, steroids, and saponins [13]. GC-MS analysis revealed the presence of bioactive alkaloid amines in the plant [14]. In our previous study, the extract of *N. lotus* leaf ameliorated the hepatotoxic effect of carbon tetrachloride (CCl₄) [15]. There is however a need to investigate the mode of action of *N. lotus* against chronic liver injury.

In this study, we investigated the effect of the ethanol extract of *N. lotus* leaf on CCl₄-induced liver fibrosis. To understand its mechanism of action, the modulatory effect of the extract on markers of liver fibrosis markers

such as α -SMA, COL4A, and TGF- β 1/SMAD signalling pathway were evaluated.

Materials and methods

Materials

TGF β 1 (E-AB-22214), COL4A1 (Cat No. E-AB-22150) monoclonal, SMAD3 (Cat. No. E-AB-40050), SMAD2 (Cat No. E-AB-32919), ACTA2 (Cat No. E-AB-16235) and MMP2 (Cat No. E-AB-13063) polyclonal antibodies were obtained from ElabScience Biotechnology Inc. Corporate (USA).

Plant collection and extraction

The leaves of *N. lotus* were collected from the Aisenwen River along Idasen-Uteh road, Owo, Ondo State, Nigeria. Leaves were rinsed, air-dried, pulverized and extracted in absolute ethanol using the maceration method as earlier reported [14]. Leaves were identified, authenticated and linked with an existing voucher number (UIH-22349).

Animal care and experimentation

Six-week-old male Wistar rats (130 \pm 13 g) were obtained for the experiment. These were housed in the experimental unit of the Animal House of the University of Medical Sciences Ondo, Nigeria. The animals were acclimatized for two weeks. The study was carried out following the NIH guidelines for animal care and use. The study was approved by the Institutional Ethical Committee of the Faculty of Life Sciences, University of Benin, Benin City Nigeria (LS19108).

Rats were divided into five groups ($n=6$). Group I served as the negative control group, Group II was the Liver fibrosis (LF) model group, and Groups III – V received 50, 100 and 200 mg/kg of the extract respectively. Doses were chosen based on our previous studies where we investigated the acute toxicity and preliminary hepatoprotective effect of the extract [15, 16]. Liver fibrosis was induced by intraperitoneal injection of 50% CCl₄ (CCl₄: Olive oil, 1:1) twice a week for 9 weeks [17]. Aside from the control group, all animals received CCl₄ twice a week for 9 weeks. Groups III–V received the extract from weeks seven to nine. The extract was reconstituted in olive oil and administered by oral gavage for five days a week on the days when CCl₄ were not administered. Group one served as the control and received distilled water instead of extract. Body weight was measured weekly throughout the experiment.

Rats were sacrificed twenty-four hours after the last CCl₄ exposure under anaesthesia (Xylazine/ketamine cocktail 20 mg/mL/50 mg/mL given at 0.1mL per 100 g b.wt.). Blood was collected via cardiac puncture, and the livers were rapidly excised. The liver collected from each animal was rinsed with 1.15% KCl, blotted and weighed.

A portion of the liver for antioxidant enzyme analysis was cut and rapidly preserved at -20 °C while the remaining portion was preserved in 10% buffered formalin for histopathology and immunohistochemical analysis. Relative liver weight was calculated as earlier reported [18]. Serum and homogenate were prepared as previously reported by Oyeyemi et al. [19].

Biochemical analysis

Serum aspartate aminotransferase (AST) and alanine aminotransaminase (ALT) were determined spectrophotometrically using Randox[®] kits. Hepatic antioxidant enzymes namely (superoxide dismutase (SOD), catalase and reduced glutathione (GSH) and lipid peroxidation were measured spectrophotometrically using previously reported methods [20–24].

Histopathology analysis

Small pieces of liver tissues preserved in 10% buffered formalin were used for histopathology analysis. Haematoxylin and eosin staining was carried out as previously described by Oyinleye et al., [25]. The liver samples were also stained using Masson's trichrome technique to show the different levels of collagen deposition and vacuolar degeneration of the liver cells [26].

Immunohistochemical analysis

Formalin-fixed paraffin-embedded specimens were cut into 4- μ m sections and mounted on positively charged slides. The slides were deparaffinized in xylene, rehydrated in descending grades of alcohol, and then washed in Tris-buffered saline. Immunohistochemical assays were performed using a DAKO immunostainer (DAKO, Carpinteria, CA) with antibodies and antigen unmasking. Slides were incubated in 0.03% hydrogen peroxide for 5 min to block endogenous peroxidase activity, followed by incubation for 20 min in a protein-blocking solution (Protein Block Serum-free solution, DAKO) to reduce nonspecific background. Envision+ reagents (DAKO) were used as a detection system. Slides were then treated for 5 min with a 3–3'-diaminobenzidine chromogen, counterstained with hematoxylin, and mounted with DPX. Appropriate negative controls for the immunostaining were prepared by omitting the primary antibody step. The measurement of immune-reactive positive expression was carried out digitally using quantification software (ImageJ Fiji). Five (5) photomicrographs were analyzed per group for each parameter.

In silico docking

Ligand preparation

The 3D structures of 26 phytochemicals identified in *N. lotus* by GC-MS [14] and two reference drugs currently

in different phases of clinical trials for the treatment of liver fibrosis were validated and retrieved from PubChem in 3D SDF file format. OpenBabel interface built in the PyRx docking tool was utilized at default settings to optimize the ligands for docking by minimizing their energy level and were converted to autodock ligand Pdbqt files in preparation for docking.

The reference drugs are Fluorofenidone and Emricasan. Fluorofenidone is a known inhibitor of TGF β 1 and it is currently in phase I of clinical trial [27]. Emricasan currently on phase II clinical trial is a pan-caspase inhibitor and double agonists of peroxisome proliferator-activated receptors alpha and gamma. The latter was selected at random since drugs with multiple targets have a higher chance of success as antifibrotic agents [28].

Protein preparation

The 3-dimensional crystal structures of each of TGF β 1 and SMAD3 proteins with PDB IDs (1IAS and 1MJS) respectively were retrieved from the Protein Data Bank in the PDB file format. The proteins were prepared for docking by removing the previously docked ligands and adding hydrogen atoms and charges using discovery studio biovia and UCSF chimera software. CastP, an online web server was used for the active site prediction of the protein 3D structures.

Molecular docking

AutoDock Vina interface on PyRx docking tool was used to perform the molecular docking studies. The protein-ligand interactions were predicted by docking the phytochemicals into the active pockets of the targets with PyRx docking software. The active pockets on the target proteins were set to be in the middle of the grid box and the docking was performed at the default setting. Macromolecule-ligand complexes were formed using Nepad++. The visualization of the binding poses in 2 and 3-D structures was performed with Discovery Studio Biovia software.

Molecular dynamic simulation

The complex (TGF- β 1/4-(4-Chlorophenyl)-2,6-diphenylpyridine complex with the best docking parameters after the post-docking analysis was selected for molecular dynamic (MD) simulation. The MD simulation was performed with the Desmond package in Schrödinger suite v2021-3 further to determine the stability of the complexes [29]. Complex preparation and all the MD simulation parameters were performed following the steps of Alturki et al. [29]. The complex was prepared for simulation using the system builder where the volumes were minimized with the steepest descent method-based protocol and the SPC water model in an

orthorhombic shape with $10 \text{ \AA} \times 10 \text{ \AA} \times 10 \text{ \AA}$ periodic boundary conditions in the P-L complex's x, y, and z-axis. Na^+ was added to the proteins to neutralize the system. OPLS2005 force field was used to minimize the complex's energy through heating at 0–300 K and equilibrium processes before the MD run. The final MD run was produced at 50 ns with 50 ps time steps, 300 K temperature and 1.01325 atm pressure following the Nose-Hoover method with an NPT ensemble [29].

Statistical analysis

Data were analysed using Statistical Package for Social Sciences (SPSS) version 23 software. Numeric data were presented as Mean \pm SD. Differences between groups were analysed with One-way ANOVA followed by the Duncan multiple Range Posthoc test. p values < 0.05 were considered significant.

Result

Body weight and relative organ weight

Body and relative organ weight changes are simple but useful indicators of toxicity. The growth and percentage body weight change in the CCl_4 model group was significantly lower than that of the control ($p < 0.05$). The groups which received CCl_4 had a lower percentage of body weight gain ($p > 0.05$) compared to the control group (Fig. 1). The relative liver weight on the other hand

was significantly higher in the CCl_4 group compared to the control ($p < 0.05$). This was however ameliorated by the extract which significantly reduced the relative liver weight relative to the negative control (Fig. 1).

Nymphaea lotus alleviated CCl_4 -induced liver injury

ALT and AST are known markers of hepatic injury. These were significantly elevated by CCl_4 compared to the negative control. Administration of the extract ameliorated the hepatic injury by significantly reducing the levels of AST ($p < 0.05$) and ALT ($p < 0.05$) to levels comparable to the negative control (Fig. 2). Histopathology analysis further revealed that CCl_4 induced liver fibrosis, severe fatty degeneration and hepatic lesions which were mitigated by the extract. Hematoxylin and eosin staining revealed severe periportal cellular infiltration, with severe diffuse hepatic necrosis and severe portal congestion in rats exposed to CCl_4 . Severe periportal cellular infiltration with moderate to severe periportal hepatic fatty degeneration and necrosis was observed in the $\text{CCl}_4 + 50$ group, severe centroacinar hepatic vacuolar degeneration and necrosis in the $\text{CCl}_4 + 100$ group and moderate-severe centroacinar hepatic vacuolar degeneration and necrosis in $\text{CCl}_4 + 200$ group (Fig. 3). Mason trichrome staining revealed no visible lesion in the control group, severe fatty degeneration of hepatocytes in liver fibrosis group, prominent periportal connective tissue, with moderate

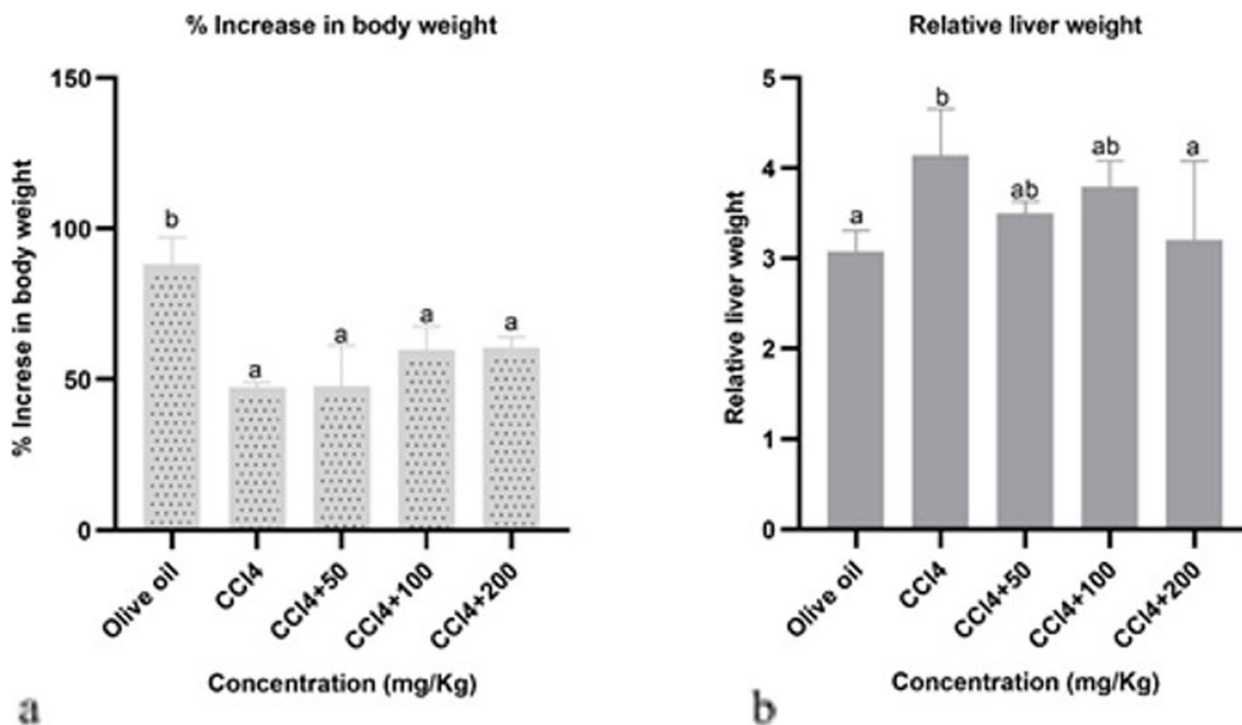


Fig. 1 Effect of the ethanol extract of *Nymphaea lotus* on (a) percentage increase in body weight) and (b) relative liver weight

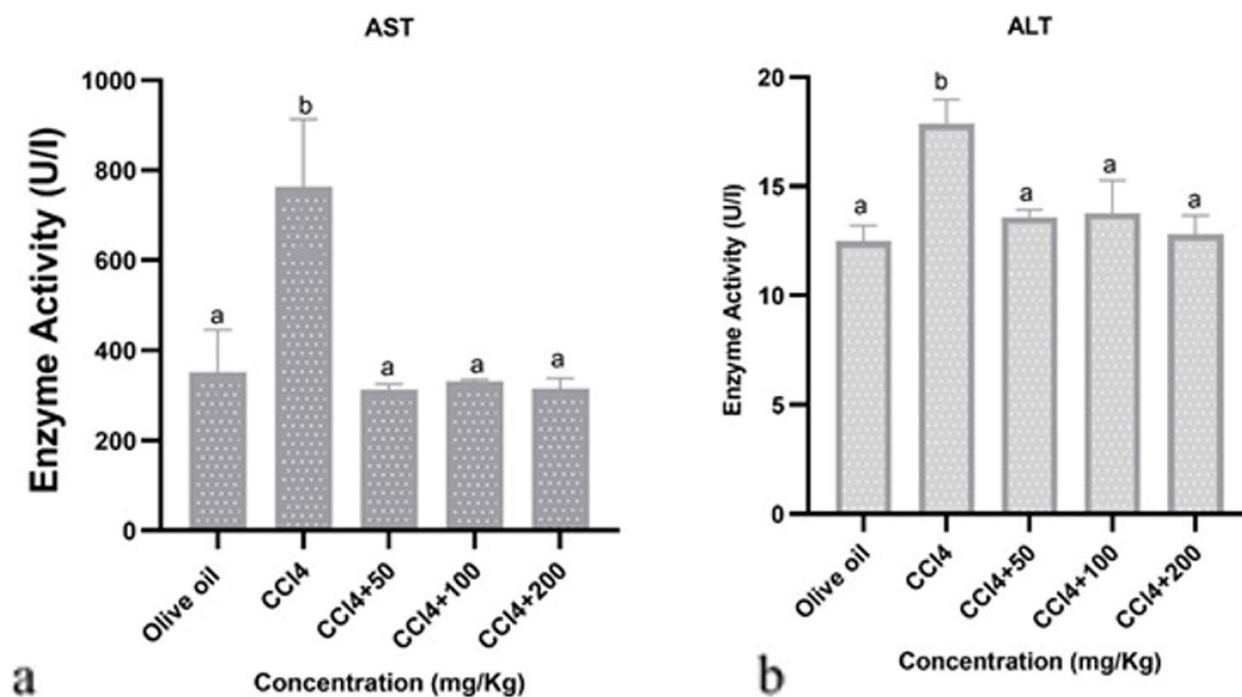


Fig. 2 Effect of the ethanol extract of *Nymphaea lotus* on (a) aspartate aminotransferase (AST) and (b) alanine aminotransaminase (ALT) in rats exposed to carbon tetrachloride (CCl₄)

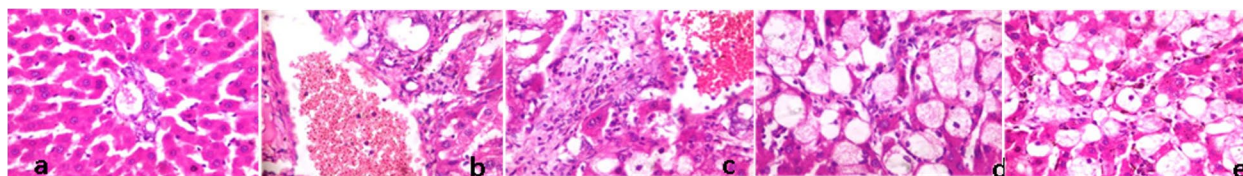


Fig. 3 Representative images of Hematoxylin and eosin staining livers exposed to carbon tetrachloride and ethanol extract of *Nymphaea lotus*. Liver section of the (a) control group showing very mild periportal cellular infiltration (b) CCl₄ model group showing severe periportal cellular infiltration, with severe diffuse hepatic necrosis and severe portal congestion (c) CCl₄+50 group showing severe periportal cellular infiltration with moderate to severe periportal hepatic fatty degeneration and necrosis (d) CCl₄+100 showing severe centroacinar hepatic vacuolar degeneration and necrosis (e) CCl₄+200 showing moderate severe centroacinar hepatic vacuolar degeneration and necrosis

diffuse fatty degeneration and necrosis of the hepatocytes in CCl₄+50 group, mild periportal fatty infiltration in CCl₄+100 group and moderate diffuse fatty degeneration of the hepatocytes in CCl₄+200 group (Fig. 4).

Effect of *Nymphaea lotus* on oxidative stress and antioxidant status

The effect of *N. lotus* extract on CCl₄-induced oxidative stress was determined by estimating the activities of antioxidant enzymes, lipid peroxidation and reduced glutathione level. CCl₄ induced oxidative stress in the animals exposed to it as evidenced by a significant reduction ($p < 0.05$) in the activities of SOD and CAT compared to the negative control (Table 1). This was however

ameliorated by extract which increased the SOD and CAT levels to a level comparable to that of the negative control. The level of GSH was also significantly ($p < 0.05$) depleted by CCl₄ which was raised by the extract ($p > 0.05$). CCl₄ similarly induced a significant increase ($p < 0.05$) in lipid peroxidation which was ameliorated by the extract (Table 1).

Nymphaea lotus modulated fibrosis-related proteins

Immunohistochemical analysis was used to investigate the expression of α -SMA, a reliable marker of liver fibrosis and HSC activation [30]. A significant increase ($p < 0.05$) in the expression of α -SMA was observed in the liver of animals in the fibrosis model group compared

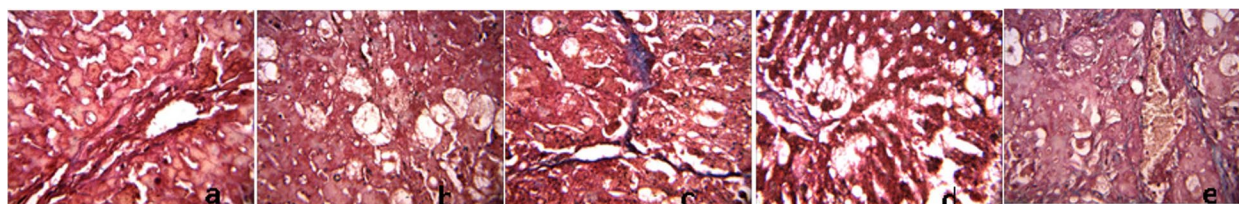


Fig. 4 Representative images of Masson's trichrome staining of rat livers exposed to carbon tetrachloride and ethanol extract of *Nymphaea lotus*. Liver section of (a) negative control group showing no visible lesion seen (b) CCl_4 group showing severe fatty degeneration of hepatocytes (c) $\text{CCl}_4 + 50$ showing prominent periportal connective tissue, with moderate diffuse fatty degeneration and necrosis of the hepatocytes (d) $\text{CCl}_4 + 100$ showing mild periportal fatty infiltration (e) $\text{CCl}_4 + 200$ showing moderate diffuse fatty degeneration of the hepatocytes

Table 1 Effect of the ethanol extract of *Nymphaea lotus* on the antioxidant status of Wistar rats exposed to carbon tetrachloride

Conc. (mg/kg)	SOD ($\mu\text{mg Protein}$)	CAT ($\mu\text{mole H}_2\text{O}_2/\text{min/mg protein}$)	GSH ($\mu\text{g/ml}$)	Lipid peroxidation ($\mu\text{M MDA/mg protein}$)
Olive oil	400.00 \pm 70.71 ^b	300.06 \pm 63.59 ^d	27.68 \pm 2.87 ^b	0.31 \pm 0.031 ^a
CCl_4	166.67 \pm 57.74 ^a	54.94 \pm 16.29 ^a	21.00 \pm 3.03 ^a	0.71 \pm 0.44 ^b
$\text{CCl}_4 + 50$	287.50 \pm 47.87 ^b	180.57 \pm 32.01 ^c	23.82 \pm 0.71 ^a	0.53 \pm 0.14 ^{ab}
$\text{CCl}_4 + 100$	333.33 \pm 76.38 ^b	134.98 \pm 29.45 ^{bc}	23.20 \pm 0.34 ^a	0.52 \pm 0.17 ^{ab}
$\text{CCl}_4 + 200$	300.00 \pm 70.71 ^b	187.27 \pm 61.69 ^c	21.63 \pm 0.34 ^a	0.48 \pm 0.09 ^{ab}

Mean value separated by Multiple Duncan Range Test

to the control group. The α -SMA-positive areas in rats treated with *N. lotus* extract were significantly smaller (Fig. 5). CCl_4 also significantly increased the expression of fibrosis-associated proteins namely; COL4A, TGF β 1, SMAD2 and SMAD3. The expression of SMAD3, TGF β 1, and COL4A was significantly ($p < 0.05$) lowered by the extract while the reduction in the expression of SMAD2 was not significant ($p > 0.05$). CCl_4 decreased the expression of MMP2 compared to the control ($p < 0.05$) which was further decreased by the extract ($p > 0.05$).

Molecular docking and interactions of compounds

The binding affinities of eight *N. lotus*-derived compounds that were retrievable from PubChem which showed higher negative binding activities to either TGF β 1 or SMAD3 compared to standard drugs are presented in Table 2. Six of the *N. lotus*-derived phytochemicals bound TGF β 1 with high affinity while five of the phytochemicals bound strongly with SMAD3. The molecular weight and formula of the compounds are presented in Table 3. Compounds with higher binding affinities than standard drugs are indicated in boldface. 4-(4-Chlorophenyl)-2,6-diphenylpyridine however had the best docking parameters. The binding pose of the phytocompounds with their corresponding receptors is presented in Fig. 6. Post-docking analysis revealed that the phytocompounds with the best binding energies exhibited good hydrogen and hydrophobic interactions

with the atoms at the binding sites of their respective receptors.

Molecular dynamics of lead compounds

Molecular dynamics (MD) simulation is essential to determine the stability and dynamic behaviour of ligands against molecular target(s). MD simulation trajectories and simulation interaction diagram produced from 50 ns run were analysed to understand the deviation and fluctuation of our selected complexes. Root mean square deviation (RMSD) value functions in the calculation of deviation in the backbone of the protein (C α , C, and N) during the MD run while the root mean square fluctuation (RMSF) analysis gives the complex variations with time evolution against each atom. TGF- β 1/4-(4-Chlorophenyl)-2,6-diphenylpyridine complex did not deviate much during the MD run. TGF- β 1 RMSD deviated from 0 to 1.8 Å initially while 4-(4-Chlorophenyl)-2,6-diphenylpyridine deviated to 1.0 Å (Fig. 7). The protein attained equilibrium at about 41 ns and was at 3.3 Å while the ligand showed 1.0 Å RMSD value at 50 ns. This is within the acceptable limit of deviation of ≤ 4 Å.

The RMSF of the TGF- β 1/4-(4-Chlorophenyl)-2,6-diphenylpyridine complex with the protein contacts with the ligand during the period of simulation is presented in Fig. 7d. The ligand interacted with GLY 286, LYS 337 and ASN 338 more than 20% of the simulation time. The radius of gyration is another indicator of the

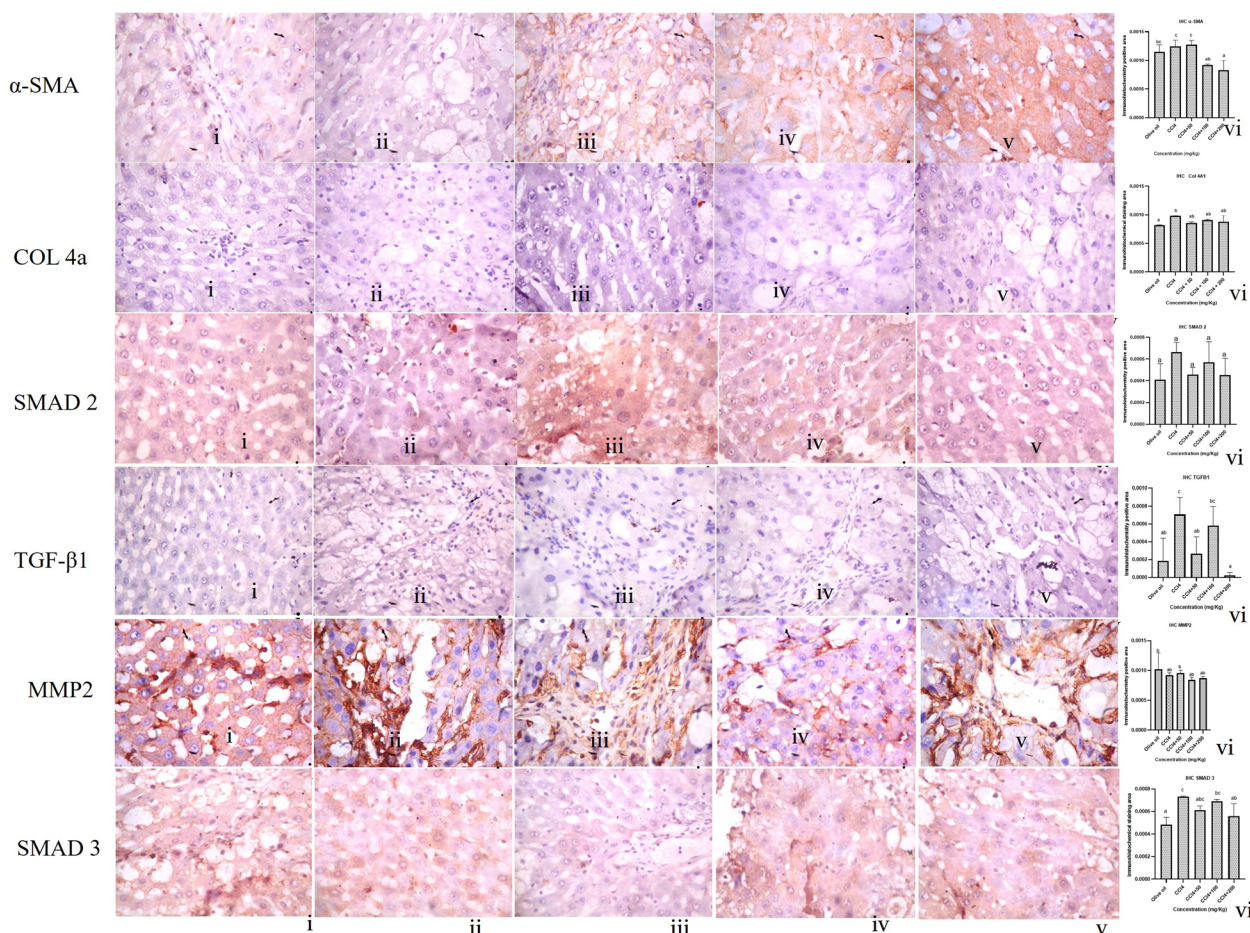
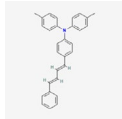
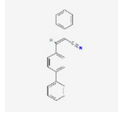
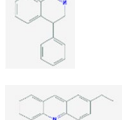
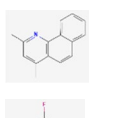
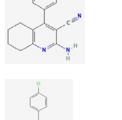
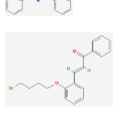

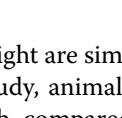


Fig. 5 Immunohistochemical representation of profibrotic markers in the liver tissue labelling with anti- α -SMA, COL 4a, SMAD2, TGF- β 1, MMP2 and SMAD3 at X400 magnification. Graph bars are presented as mean \pm standard deviation. Mean values are separated by Duncan Multiple Range Test. Immunohistochemical staining patterns in (i) Control; (ii) CCl₄ alone; (iii) CCl₄ + ENL (50 mg/kg); (iv) CCl₄ + ENL (100 mg/kg); (v) CCl₄ + ENL (200 mg/kg) (vi) Graphical representation of immunohistochemistry positive area

Table 2 The binding affinity of compounds identified in *N. lotus* for TGF β 1 and SMAD3

S/N	Ligands	Pubchem CID	Binding energy (kcal/mol)	
			TGF- β 1 (1IAS)	SMAD3 (1MJS)
1.	benzenamine, 4-methyl-N-(4-methylphenyl)-N-[4-[4-phenyl-1,3-butadien-1-yl]phenyl]-	14,618,324	-8.4	-7.5
2.	Benzene, 1-phenyl-4-(2-cyano-2-phenylethenyl)	5,378,125	-9.1	-8.0
3.	4-Phenyl-3,4-dihydroisoquinoline	610,131	-8.2	-7.0
4.	2-Ethylacridine	610,161	-8.8	-6.4
5.	Benzo[h]quinoline, 2,4-dimethyl-	610,182	-9.1	-6.8
6.	Quinoline-3-carbonitrile, 5,6,7,8-tetrahydro-2-amino-4-(4-fluorophenyl)-	622,529	-7.2	-7.4
7.	4-(4-Chlorophenyl)-2,6-diphenylpyridine	631,072	-11.6	-8.2
8.	(E)-2-bromobutyloxchalcone	91,733,949	-8.4	-6.2
	<i>Reference Drugs</i>			
	<i>Fluorfenidone</i>	11,851,183	-8.3	-5.8
	<i>Emricasan</i>	12,000,240	-8.4	-6.8

Table 3 Molecular weight, formula and structure of compounds with higher binding affinities to the protein targets

S/No	Compounds	Molecular weight (g/mol)	Molecular formula	Structure
1.	benzenamine, 4-methyl-N-(4-methylphenyl)-N-[4-[4-phenyl-1,3-butadien-1-yl]phenyl]-	401.5	C ₃₀ H ₂₇ N	
2.	Benzene, 1-phenyl-4-(2-cyano-2-phenylethenyl)	281.3	C ₂₁ H ₁₅ N	
3.	4-Phenyl-3,4-dihydroisoquinoline	207.27	C ₁₅ H ₁₃ N	
4.	2-Ethylacridine	207.27	C ₁₅ H ₁₃ N	
5.	Benzo[h]quinoline, 2,4-dimethyl-	207.27	C ₁₅ H ₁₃ N	
6.	Quinoline-3-carbonitrile, 5,6,7,8-tetrahydro-2-amino-4-(4-fluorophenyl)-	267.3	C ₁₆ H ₁₄ FN ₃	
7.	4-(4-Chlorophenyl)-2,6-diphenylpyridine	341.8	C ₂₃ H ₁₆ ClN	
8.	(E)-2-bromobutyloxychalcone	359.3	C ₁₉ H ₁₉ BrO ₂	

total size of the chain molecule which is employed to evaluate the compactness manner and flexibility of the protein in a biological environment during the simulation production. The low value of Rg indicates a more rigid structure shown in this study.

Discussion

Liver fibrosis is a pathological state, arising from different aetiologies, whose burden increases end-stage liver diseases, mortality and extrahepatic diseases [2]. There are currently limited treatment options for liver fibrosis. However, medicinal plants used for the traditional management of liver diseases have shown potential as antifibrotic agents. *N. lotus* is a medicinal plant used traditionally for the management of liver diseases [15]. In our previous studies, we reported that it ameliorates CCl₄-induced chronic liver injury via inhibition of oxidative stress activity [15] and has anti-inflammatory effects [14]. In this study, we proceeded to study its

mode of action in CCl₄-induced liver fibrosis in Wistar rats.

Body weight changes and relative organ weight are simple but useful markers of toxicity. In this study, animals in the CCl₄ group exhibited slower growth compared to the other groups, as indicated by a lower percentage increase in body weight. This is an indication that hepatic fibrosis was possibly successfully induced [31]. AST and ALT are known markers of hepatic dysfunction. They are usually in high concentration in the liver, an increase in their serum or plasma concentration is however an indication of hepatic injury [32]. The increase in the activities of AST and ALT in CCl₄-exposed rats in this study indicates the toxicity of CCl₄ to the liver of the cells exposed to it. The decline in the levels of AST and ALT in rats exposed to CCl₄ and the extract showed that the extract mitigated CCl₄-induced liver dysfunction. This is in line with our previous report [15]. The increase in the level of these enzymes is a result of CCl₄-induced oxidative stress which is evidenced by the observed increase in lipid peroxidation products measured as Malondialdehyde

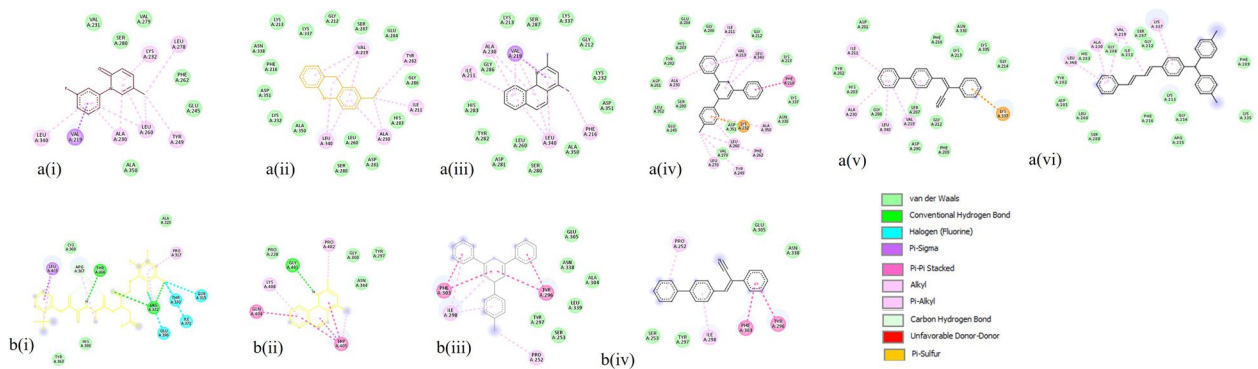


Fig. 6 2D Interactions of standard drugs and phytochemicals with their corresponding target a(i) TGFβ1-Fluorfenidone (reference) a(ii) TGFβ1-2-Ethylacridine a(iii) TGFβ1-Benzo[h]quinoline, 2,4-dimethyl- a(iv) TGFβ1-4-(4-Chlorophenyl)-2,6-diphenylpyridine a(v) TGFβ1-Benzene, 1-phenyl-4-(2-cyano-2-phenylethenyl) a(vi) TGFβ1-benzenamine, 4-methyl-N-(4-methylphenyl)-N-[4-[4-phenyl-1,3-butadien – 1-yl]phenyl]- b(i) SMAD3-Emricasan (reference) b(ii) SMAD3-Benzo[h]quinoline, 2,4-dimethyl- b(iii) SMAD3-4-(4-Chlorophenyl)-2,6-diphenylpyridine b(iv) SMAD3-Benzene, 1-phenyl-4-(2-cyano-2-phenylethenyl)

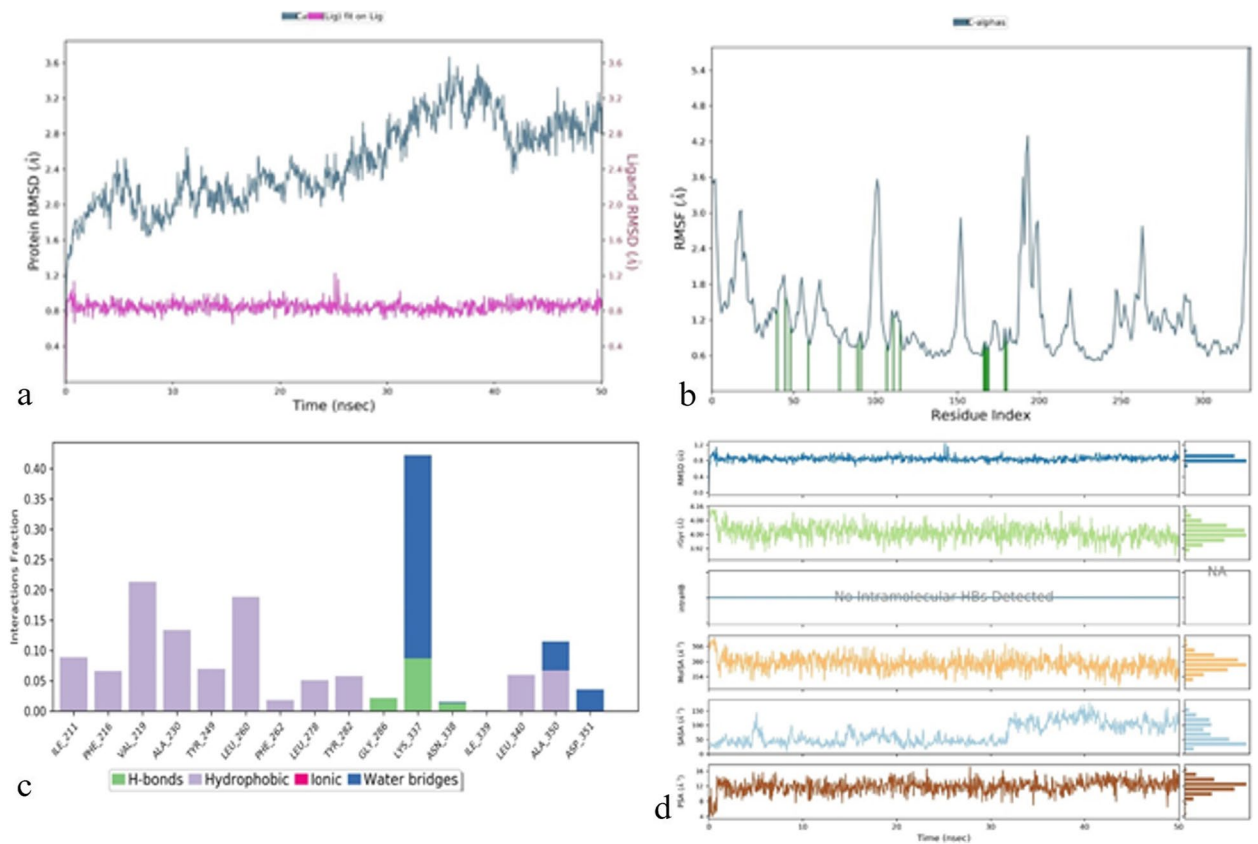


Fig. 7 Molecular dynamic simulation of protein (TGF-β1) – 4-(4-Chlorophenyl)-2,6-diphenylpyridine (a) RMSD plots of molecular dynamics (MD) simulation of ligands complexed to TGF-β1 (b) Per residue root mean square fluctuations (RMSF) plots of molecular dynamics (MD) simulation of ligands complexed to TGF-β1 (c) protein ligand interaction of the ligand with TGF-β1 (d) The backbone-root mean square deviation (RMSD) plots, the radius of gyration (rGyr), intramolecular Hydrogen bond (intraHB), molecular surface area (molSA), surface accessible surface area (SASA) plots and polar surface area (PSA) of molecular dynamics simulation of ligand complexed to TGF-β1

(MDA) and depletion of the antioxidant enzymes activities. The extract in this study mitigated oxidative stress. Oxidative stress plays a significant role in the fibrogenic process. It is involved in the initiation of hepatic fibrosis and mediates molecular and cellular events involved in the progression of liver fibrosis [33]. Increased reactive oxygen species (ROS) mediate signalling pathways which lead to the activation of HSC, increased collagen deposition and dysregulation of the ECM composition [34, 35]. Attenuation of oxidative stress is thus one of the strategies employed by *N. lotus* to halt the fibrogenic process.

The ameliorative effect of the extract on liver fibrosis was further revealed by the histopathological analysis which revealed attenuation of liver injury. An increase in collagen deposition is a hallmark of liver fibrosis [36]. CCl₄ increased collagen deposit in the liver which was ameliorated by the extract. Markers of liver fibrosis namely Collagen 1 and α -SMA [10, 37] were also mitigated in this study. These all indicated that *N. lotus* mitigated CCl₄-induced liver fibrosis. α -SMA is a marker of HSC activation, an important event in the initiation of liver fibrosis [38]. This shows that the extract inhibited early fibrosis by inhibiting the accumulation of collagen and the expression of α -SMA which would have led to HSC activation [39, 40]. Thus, *N. lotus* attenuated liver fibrosis via inhibition of HSC activation.

The TGF β /SMAD signal is activated by oxidative stress and proinflammatory cytokines leading to the trans-differentiation of HSC [41]. TGF β 1 is a profibrogenic cytokine and a key driver of HSC activation and HSC-mediated ECM production [42]. It plays a critical role in the progression of hepatic fibrosis by activating the downstream mediators – SMAD2 and SMAD3 [43, 44]. SMAD3 regulates the transcription of fibrogenic genes, including α -SMA and pro-collagen type I [45]. Our present study showed that *N. lotus* inhibited the expression of TGF β 1 and SMAD 3. This implies the inhibitory effect of *N. lotus* extract on the TGF β /SMAD signal pathway, a mechanism that probably underlies its anti-fibrotic effect.

Following the activation of HSC, there is an increase in collagen secretion and deposition which leads to hepatic fibrosis [46]. Collagen 4 (COL4A) is one of the clinical indicators for assessing the degree of hepatic fibrosis [47]. Extensive deposition of COL4A could lead to portal and sinus fibrosis [46]. Increased MMP2 level is associated with increased collagen synthesis and liver fibrosis [48]. In this study, *N. lotus* regulated MMP2 expression and inhibited the deposition of Collagen, thereby inhibiting liver fibrosis.

The antifibrotic effect of *N. lotus* was further confirmed by the *in silico* analysis. This shows that *N. lotus* is rich in phytochemicals that can modulate the TGF β /SMAD signalling pathway. *N. lotus*-derived phytochemicals

thus worked synergistically to inhibit liver fibrosis. 4-(4-Chlorophenyl)-2,6-diphenylpyridine especially showed a high binding affinity with TGF β 1 and SMAD3. It is thus a compound that could be a target for isolation to serve as a lead for hepatic fibrosis drug development.

Conclusion

This study demonstrated that *N. lotus* exerted a protective effect against liver fibrosis. *N. lotus* inhibited CCl₄-induced liver fibrosis via inhibition of oxidative stress and TGF β /SMAD signalling pathway. Of the *N. lotus*-derived phytochemicals, 4-(4-Chlorophenyl)-2,6-diphenylpyridine showed a high binding affinity with TGF β 1 and SMAD3. This compound can be isolated to serve as a lead for the production of drug for liver fibrosis.

Abbreviations

CCl ₄	carbon tetrachloride
ALT	alanine aminotransaminase
AST	aspartate aminotransferase
MDA	Malondialdehyde
SOD	superoxide dismutase
GSH	reduced glutathione
α -SMA	alpha-smooth muscle actin
COL4A	Collagen-4
TGF β 1	Transforming growth factor- β 1
SMAD2	Mothers against decapentaplegic homolog 2
SMAD3	Mothers against decapentaplegic homolog 3
MMP2	Matrix metalloproteinase 2
TIMP2	Tissue Inhibitor of Metalloproteinase 2
HSC	Hepatic stellate cells
ECM	Extracellular matrix
GC-MS	Gas chromatography/Mass spectrometry
PDB	Protein Data Bank
MD	Molecular dynamics
SPSS	Statistical Package for the Social Sciences
RSMD	Root mean square deviation
RMSF	Root mean square fluctuation
GLY	Glycine
LYS	Lysine
ASN	Asparagine

Acknowledgements

The authors acknowledge the management of the University of Medical Sciences, Ondo, Nigeria for providing the needed facilities for this study.

Authors' contributions

ITO – conceived and designed the experiment, was involved in the experiment and drafting of the manuscript, IAA – collected the plant and was involved in the experiment, KAS – conducted the *in silico* analysis and contributed to drafting the manuscript, ITA prepared tissue sections and analyzed both the histopathology and immunohistochemical slides, EWN contributed to the analysis of immunohistochemical slides and drafting of manuscript.

Funding

This work was funded by the Joint University of Medical Sciences and Centre of Excellence in Reproductive Health and Innovation grant awarded to ITO. The funder played no role in the study design; in the collection, analysis and interpretation of data; in the writing of the report; and in the decision to submit this article for publication.

Availability of data and materials

No datasets were generated or analysed during the current study.

Declarations

Ethics approval and consent to participate

The study was carried out in line with the NIH guidelines for animal care and use. The study was approved by the Institutional Ethical Committee of the Faculty of Life Sciences, University of Benin, Benin City Nigeria (LS19108).

Consent for publication

Not Applicable.

Competing interests

The authors declare no competing interests.

Author details

¹Department of Biosciences and Biotechnology, University of Medical Sciences, Ondo City 351104, Nigeria. ²Department of Microbiology, University of Medical Sciences, Ondo City 351104, Nigeria. ³Department of Medical Laboratory Sciences, University College Hospital, Ibadan 200212, Nigeria. ⁴Department of Physiology, Babcock University, Ilishan-Remo 121103, Nigeria. ⁵Department of Biomedical Sciences, University of Wolverhampton, Wolverhampton, UK.

Received: 13 May 2024 Accepted: 27 August 2024

Published online: 27 September 2024

References

- Devarbhavi H, Asrani SK, Arab JP, Nartey YA, Pose E, Kamath PS. Global burden of liver disease: 2023 update. *J Hepatol.* 2023;79:516–37.
- Parola M, Pinzani M. Liver fibrosis in NAFLD/NASH: from pathophysiology towards diagnostic and therapeutic strategies. *Mol Aspects Med.* 2024;95:101231.
- Rockey DC, Friedman SL. Fibrosis regression after eradication of hepatitis C virus - from bench to bedside. *Gastroenterology.* 2021;160:1502. /pmc/articles/PMC8601597.
- Wang Y, Jiao L, Qiang C, Chen C, Shen Z, Ding F, et al. The role of matrix metalloproteinase 9 in fibrosis diseases and its molecular mechanisms. *Biomed Pharmacother.* 2024;171:116116.
- Weiskirchen R. Hepatoprotective and anti-fibrotic agents: It's time to take the next step. *Front Pharmacol.* 2016;6:303. <https://pubmed.ncbi.nlm.nih.gov/26779021/>
- Zein N, Yassin F, Makled S, Aloataibi SS, Albogami SM, Mostafa-Hedeab G et al. Oral supplementation of policosanol alleviates carbon tetrachloride-induced liver fibrosis in rats. *Biomed Pharmacother.* 2022;150:113020. <https://linkinghub.elsevier.com/retrieve/pii/S075333222004097>
- Gandhi CR. Oxidative stress and hepatic stellate cells: A paradoxical relationship. *Trends cell Mol Biol.* 2012;7:1 /pmc/articles/PMC5051570/.
- Gough NR, Xiang X, Mishra L. TGF- β signaling in liver, pancreas, and gastrointestinal diseases and cancer. *Gastroenterology.* 2021;161:434–e45215.
- Hu HH, Chen DQ, Wang YN, Feng YL, Cao G, Vaziri ND et al. New insights into TGF- β /Smad signaling in tissue fibrosis. *Chem Biol Interact.* 2018;292:76–83. <https://pubmed.ncbi.nlm.nih.gov/30017632/>
- Zhang L, Liu C, Yin L, Huang C, Fan S. Mangiferin relieves CCl₄-induced liver fibrosis in mice. *Sci Rep.* 2023;13:1–9. <https://pubmed.ncbi.nlm.nih.gov/36914687/>
- Wang Z, Sun P, Zhao T, Cao J, Liu Y, Khan A, et al. E Se tea extract ameliorates CCl₄ induced liver fibrosis via regulating Nrf2/NF- κ B/TGF- β 1/Smad pathway. *Phytomedicine.* 2023;115:154854.
- Ebrahimi H, Naderian M, Sohrabpour AA. New concepts on reversibility and targeting of liver fibrosis; A review article. *Middle East J Dig Dis.* 2018;10:133 /pmc/articles/PMC6119836/.
- Oyeyemi IT, Bakare AA. Genotoxic and anti-genotoxic effect of aqueous extracts of *Spondias mombin* L., *Nymphaea lotus* L. and *Luffa cylindrica* L. on *Allium cepa* root tip cells. *Caryologia.* 2013;66:360–7. <http://www.tandfonline.com/doi/abs/https://doi.org/10.1080/00087114.2013.857829>
- Oyeyemi IT, Adewole KE, Gyebi GA. In silico prediction of the possible antidiabetic and anti-inflammatory targets of *Nymphaea lotus*-derived phytochemicals and mechanistic insights by molecular dynamics simulations. *J Biomol Struct Dyn.* 2023;1–17. <https://www.tandfonline.com/doi/abs/https://doi.org/10.1080/07391102.2023.2166591>
- Oyeyemi IT, Akanni OO, Adaramoye OA, Bakare AA. Methanol extract of *Nymphaea lotus* ameliorates carbon tetrachloride-induced chronic liver injury in rats via inhibition of oxidative stress. *J Basic Clin Physiol Pharmacol.* 2017;28:43–50. <https://www.degruyter.com/document/doi/https://doi.org/10.1515/jbcpp-2016-0029/html>
- Oyeyemi IT, Yekeen OM, Odusina PO, Ologun TM, Ogbaide OM, Olaleye OI et al. Genotoxicity and antigenotoxicity study of aqueous and hydro-methanol extracts of *Spondias mombin* L., *Nymphaea lotus* L. and *Luffa cylindrica* L. using animal bioassays. *Interdiscip Toxicol.* 2015;8:184–92. <https://pubmed.ncbi.nlm.nih.gov/27486380/>
- Li J, Hu R, Xu S, Li Y, Qin Y, Wu Q et al. Xiaochaihutang attenuates liver fibrosis by activation of Nrf2 pathway in rats. *Biomed Pharmacother.* 2017;96:847–53. <https://pubmed.ncbi.nlm.nih.gov/29078262/>
- Bakare AA, Akpofure A, Gbadebo AM, Fagbenro OS, Oyeyemi IT. Aqueous extract of *Moringa oleifera* Lam. induced mitodepression and chromosomal aberration in *Allium cepa*, and reproductive genotoxicity in male mice. *Adv Tradit Med.* 2022;22:685–95. <https://link.springer.com/article/https://doi.org/10.1007/s13596-021-00564-9>
- Oyeyemi IT, Akanni OO, Adaramoye OA, Bakare AA. Hepatoprotective effect of the methanol extract of *Luffa cylindrica* fruit on carbon-tetrachloride induced chronic liver injury. *Acta Biol Szeged.* 2022;66:150–5. <https://abs.bibl.u-szeged.hu/index.php/abs/article/view/3348>
- Misra HP, Fridovich I. The role of superoxide anion in the autoxidation of epinephrine and a simple assay for superoxide dismutase. *J Biol Chem.* 1972;247:3170–5. <https://pubmed.ncbi.nlm.nih.gov/4623845/>
- Clairborne A. Catalase activity. In: Greenwald RA, editor. *CRC Handb methods Oxyg Radic Res.* Boca Raton: CRC Press; 1985. pp. 283–4. [https://www.scirp.org/\(S\(351jmbntvnsjt1aadkpozje\)\)/reference/ReferencesPapers.aspx?ReferenceID=796054](https://www.scirp.org/(S(351jmbntvnsjt1aadkpozje))/reference/ReferencesPapers.aspx?ReferenceID=796054)
- Beutler E, Duron O, Kelly BM. Improved method for determination of blood glutathione. *J Clin Med.* 1963;61:882–90.
- Rice-Evans C, Omorphos SC, Baysal E. Sick cell membranes and oxidative damage. *Biochem J.* 1986;237:265–9. <https://pubmed.ncbi.nlm.nih.gov/3800879/>
- Ádám-Vizi V, Seregi A. Receptor independent stimulatory effect of noradrenaline on Na,K-ATPase in rat brain homogenate: role of lipid peroxidation. *Biochem Pharmacol.* 1982;31:2231–6.
- Oyinleye OE, Adeniran SA, Ogunsuyi OM, Oyeyemi IT, Bakare AA. Genetic and reproductive toxicity of aqueous extracts of *Telfairia occidentalis* (Hook F.), *Vernonia amygdalina* and their combination on the testicular cells of male mice. *Adv Tradit Med.* 2021;21:759–65. <https://link.springer.com/article/10.1007/s13596-020-00507-w>
- Suvik A, Effendy A. The use of modified Masson's trichrome staining in collagen evaluation in wound healing study. *Malaysian J Vet Res.* 2012;3:39–47.
- Tan Z, Sun H, Xue T, Gan C, Liu H, Xie Y et al. Liver fibrosis: Therapeutic targets and advances in drug therapy. *Front cell Dev Biol.* 2021;9. <https://pubmed.ncbi.nlm.nih.gov/34621747/>
- Shan L, Wang F, Zhai D, Meng X, Liu J, Lv X. New drugs for hepatic fibrosis. *Front Pharmacol.* 2022;13:2003.
- Alturki NA, Mashraqi MM, Alzamami A, Alghamdi YS, Alharthi AA, Asiri SA, et al. In-silico screening and molecular dynamics simulation of drug bank experimental compounds against SARS-CoV-2. *Molecules.* 2022;27:1–12.
- Liu D, Qin H, Yang B, Du B, Yun X. Oridonin ameliorates carbon tetrachloride-induced liver fibrosis in mice through inhibition of the NLRP3 inflammasome. *Drug Dev Res.* 2020;81:526–33. <https://onlinelibrary.wiley.com/doi/full/10.1002/ddr.21649>
- Zhang Y, Zhao M, Liu Y, Liu T, Zhao C, Wang M. Investigation of the therapeutic effect of Yinchen Wuling Powder on CCl₄-induced hepatic fibrosis in rats by 1H NMR and MS-based metabolomics analysis. *J Pharm Biomed Anal.* 2021;200:114073. <https://linkinghub.elsevier.com/retrieve/pii/S0731708521001849>
- Farrell AM, Magliano DJ, Shaw JE, Thompson AJ, Croagh C, Ryan MC et al. A problem of proportions: estimates of metabolic associated fatty liver disease and liver fibrosis in Australian adults in the nationwide 2012 AusDiab Study. *Sci Reports* 2022 12:1. 2022;12:1–7. <https://www.nature.com/articles/s41598-022-05168-0>
- Sanchez-Valle V, Chavez-Tapia C, Uribe N, Mendez-Sanchez M. N. Role of oxidative stress and molecular changes in liver fibrosis: A review. *Curr*

- Med Chem. 2012;19:4850–60. <https://pubmed.ncbi.nlm.nih.gov/22709007/>
34. Lemos LMS, Martins TB, Tanajura GH, Gazoni VF, Bonaldo J, Strada CL, et al. Evaluation of antiulcer activity of chromanone fraction from *Calophyllum brasiliense* Camb. *J Ethnopharmacol.* 2012;141:432–9.
 35. Zhao Y, Zhao M, Wang Z, Zhao C, Zhang Y, Wang M. Danggui Shaoyao San: Chemical characterization and inhibition of oxidative stress and inflammation to treat CCl₄-induced hepatic fibrosis. *J Ethnopharmacol.* 2024;318:116870. <https://linkinghub.elsevier.com/retrieve/pii/S0378874123007389>
 36. Xue X, Zhao X, Wang J, Wang C, Ma C, Zhang Y, et al. Carthami flos extract against carbon tetrachloride-induced liver fibrosis via alleviating angiogenesis in mice. *Phytomedicine.* 2023;108:154517.
 37. Wu S, Liu L, Yang S, Kuang G, Yin X, Wang Y et al. Paeonol alleviates CCl₄-induced liver fibrosis through suppression of hepatic stellate cells activation via inhibiting the TGF- β /Smad3 signaling. *Immunopharmacol Immunotoxicol.* 2019;41:438–45. <https://www.tandfonline.com/doi/full/https://doi.org/10.1080/08923973.2019.1613427>
 38. Rahman MM, Shahab NB, Miah P, Rahaman MM, Kabir AU, Subhan N, et al. Polyphenol-rich leaf of *Aphanamixis polystachya* averts liver inflammation, fibrogenesis and oxidative stress in ovariectomized Long-Evans rats. *Biomed Pharmacother.* 2021;138:111530.
 39. Zhao Y, Liu X, Ding C, Zheng Y, Zhu H, Cheng Z et al. *Aronia melanocarpa* polysaccharide ameliorates liver fibrosis through TGF- β 1-mediated the activation of PI3K/AKT pathway and modulating gut microbiota. *J Pharmacol Sci.* 2022;150:289–300. <https://linkinghub.elsevier.com/retrieve/pii/S1347861322000767>
 40. Yang X, Ji W, Zhou Z, Wang J, Cui Z, Pan X, et al. *Dendrobium officinale* polysaccharide regulated hepatic stellate cells activation and liver fibrosis by inhibiting the SMO/Gli 1 pathway. *J Funct Foods.* 2024;112:105960.
 41. Fabregat I, Moreno-Càceres J, Sánchez A, Dooley S, Dewidar B, Giannelli G et al. TGF- β signalling and liver disease. *FEBS J.* 2016;283:2219–32. <https://onlinelibrary.wiley.com/doi/full/10.1111/febs.13665>
 42. Dewidar B, Meyer C, Dooley S, Meindl-Beinker N. TGF- β in hepatic stellate cell activation and liver fibrogenesis—updated 2019. *Cells.* 2019;8. <https://pubmed.ncbi.nlm.nih.gov/31718044/>
 43. Xu F, Liu C, Zhou D, Zhang L. TGF- β /SMAD pathway and its regulation in hepatic fibrosis. *J Histochem Cytochem.* 2016;64:157–67. <http://journals.sagepub.com/doi/10.1369/0022155415627681>
 44. Xia Y, Luo Q, Gao Q, Huang C, Chen P, Zou Y et al. SIRT1 activation ameliorates rhesus monkey liver fibrosis by inhibiting the TGF- β /smad signaling pathway. *Chem Biol Interact.* 2024;110979. <https://linkinghub.elsevier.com/retrieve/pii/S000927972400125X>
 45. Feng XH, Derynck R. Specificity and versatility in Tgf-beta signaling through Smads. *Annu Rev Cell Dev Biol.* 2005;21:659–93. <https://pubmed.ncbi.nlm.nih.gov/16212511/>
 46. Huang W, Zheng Y, Feng H, Ni L, Ruan Y, fang, Zou Xxing et al. Total phenolic extract of *Euscaphis konishii hayata* Pericarp attenuates carbon tetrachloride (CCl₄)-induced liver fibrosis in mice. *Biomed Pharmacother.* 2020;125:109932. <https://linkinghub.elsevier.com/retrieve/pii/S0753332220301220>
 47. Shamkhi FB, Abdullah F, Abbudi AL, Alrekabi MH, Hamzah MI. The role of serum type IV collagen and serum procollagen type III (PIIINP) as biomarkers for the detection and staging of liver fibrosis in a sample of Iraqi patients with chronic liver disease. *J Pharm Negat Results.* 2022;13:93–9. <https://pnjournal.com/index.php/home/article/view/1438>
 48. Zhan J, Hu T, Shen J, Yang G, Ho C, Li S. Pterostilbene is more efficacious than hydroxystilbenes in protecting liver fibrogenesis in a carbon tetrachloride-induced rat model. *J Funct Food.* 2021;84:104604. <https://www.sciencedirect.com/science/article/pii/S175646462100253X>

Publisher's note

Springer Nature remains neutral with regard to jurisdictional claims in published maps and institutional affiliations.